

Modelling and Simulations of Nanostructures for Shipley SPR505A Resist using PRIME Process

K.I. Arshak, M. Mihov, A. Arshak*, D. McDonagh** and M. Pomeroy*

Electronic & Computer Engineering Department, University of Limerick, Limerick, Ireland.

** Physics Department, University of Limerick, Limerick, Ireland.*

*** Integrated Devices Technology Inc., 11555 Medlock Bridge, Rd., Suite 170, Duluth, GA 30096, USA*

** Material Science Dept, University of Limerick, Limerick, Ireland*

E. mail: Khalil.Arshak@ul.ie (K. I. Arshak)

Abstract

The Positive Resist Image by dry Etching (PRIME) process is a high resolution lithography system incorporating electron beam exposure, silylation and dry development. The process steps in PRIME with Shipley SPR505A resist have been modeled and simulations of nanostructures (50nm lines/spaces, 30nm single line) has been presented. The silylation process step in PRIME with SPR505A resist has been experimentally characterized using FT-IR spectroscopy.

1. Introduction

Conventional optical lithography still remains the main workhouse of the semiconductor industry even in the sub quarter μm region, as the critical dimensions of semiconductor devices shrink towards $0.18\mu\text{m}$ and below [1]. Several improvements in the optical lithography have been achieved over the past few years: lowering the exposing wavelength to 248nm (KrF), 193nm (ArF) and 155nm (F_2). Improvements in the photoresist chemistry were also made leading to development of acid-catalysed resists sensitive to the above wavelengths. Introducing of anti reflective coatings (ARC) in addition to numerous optical techniques such as phase-shift masks, off-axis illumination and optical proximity corrections (OPC), had made possible to print such dimensions.

Top Surface Imaging (TSI) processes are an attractive alternative suitable for nanostructure fabrications [2]. The Positive Resist Image by dry Etching (PRIME) process is a high resolution single layer lithography system incorporating electron beam exposure, silylation and dry development [3]. The surface imaging eliminates the effects of nonplanar wafer topography and e-beam proximity effects, while the anisotropic plasma etching produces very steep resist profiles resulting in nanometer features.

2. PRIME Process Scheme

The PRIME process diagram is shown in Fig.1. The electron beam exposure (i) crosslinks the photo-active compound (PAC) with the novolak chains in the resist producing an ester, while the consequent near UV flood exposure (ii) converts PAC to indene carboxylic acid (ICA). During the liquid-phase silylation (iii), the silicon is selectively incorporated in e-beam unexposed regions, thus forming a SiO_2 layer at the dry O_2 development process (iv).

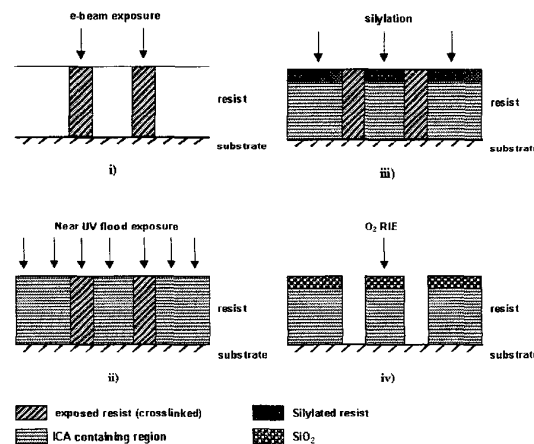


Fig. 1. PRIME process diagram.

3. Modelling of PRIME Process

The four PRIME process steps have been modeled and simulations of 50nm lines/spaces gratings and 30nm single line have been presented. The simulated resist is I-line Shipley SPR505A, a standard DNQ/novolak based resist (m-cresol formaldehyde resins), with thickness of $0.5\mu\text{m}$.

The simulation of e-beam exposure was performed using SAMPLE [4], which implements Monte Carlo technique to calculate the trajectories of large number of electrons (20K) and determines the energy deposited profile in the resist using Bethe energy loss formula. As the original settings in the program are fixed to a polymer-based resist (PMMA), several modifications in the source code were made to account for a DNQ/novolak based resist Shipley SPR505A. Fig.2 shows the simulated absorbed energy density distribution through the resist using a 0.02 μm Gaussian shaped beam at 50KeV accelerated voltage with a dose of 250 $\mu\text{C}/\text{cm}^2$.

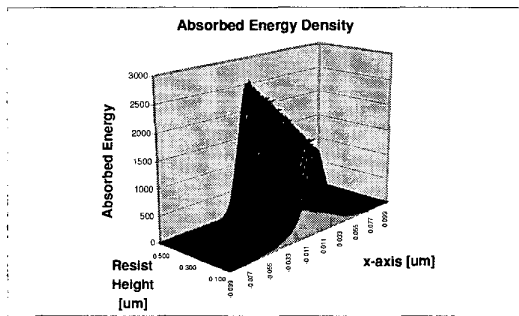


Fig.2: Simulated absorbed energy density distribution through the resist after e-beam exposure.

The e-beam exposure in DNQ/novolak resists promotes crosslinking between the PAC and the novolak chains in the exposed regions. The deposited energy density distribution profile is used to predict the crosslinked region and the ester formed as described previously [5]. Figure 3 shows a surface plot of the calculated normalised ester concentration in the resist after e-beam exposure.

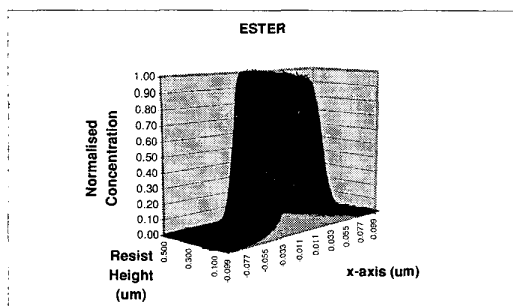


Fig.3: ESTER Concentration after e-beam exposure.

The near UV flood exposure (I-line, 365nm) was simulated with implementing Dill's model for the photochemical kinetics [6] and Mack's model for the standing wave intensity distribution [7].

During the NUV exposure, the remaining PAC is converted to ICA mostly in the resist surface areas. The optical exposure parameters, i.e. Dill A, B and C, have been measured experimentally for Shipley SPR505A resist under I-line exposure ($A=0.56\mu\text{m}^{-1}$, $B=0.039\mu\text{m}^{-1}$, $C=0.016\text{cm}^2/\text{mJ}$) and used in the simulations.

The postexposure bake, which attenuates the standing waves presented in the PAC concentration due to the monochromatic nature of the second exposure, was modeled with implementing Mack's diffusion model [8]. The value of the characteristic diffusion length was set to be 0.0051 nm^2/s for SPR505A resist, baked at 110 $^{\circ}\text{C}$ for 60 sec on hotplate [9]. The simulated PAC concentration after e-beam & NUV exposure (365nm, dose 50 mJ/cm^2) and after post-exposure bake is shown in Figure 4 and Figure 5.

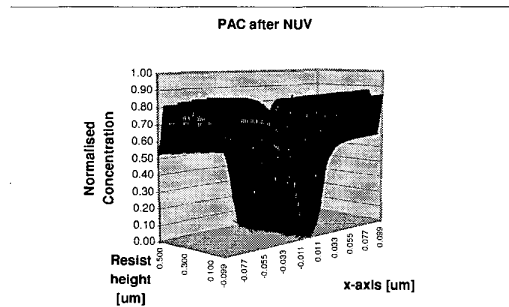


Fig.4: Simulated PAC concentration after NUV flood exposure.

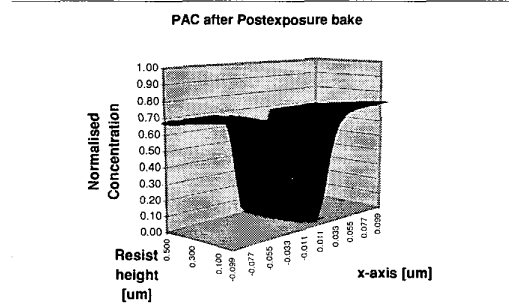


Fig.5: Simulated PAC concentration after postexposure bake.

During the silylation step, the crosslinked regions inhibit diffusion of silicon, while the ICA containing areas enhance the silicon incorporation. The silylation step was modeled using the DESIM silylation model [10], originally written for the two compound DESIRE system. Since the resist in PRIME process contains three compounds after the exposures, the DESIM model was extended using a linear interpolation scheme as described previously [5].

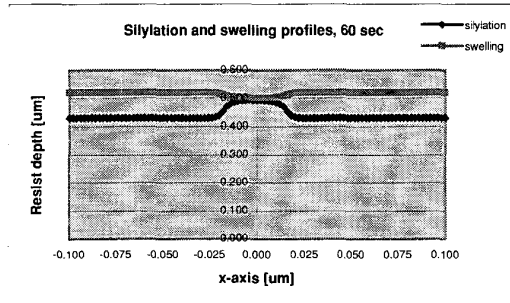


Fig.6: Silicon incorporation after 60 sec silylation.

The DESIM silylation rate model takes into account the diffusion of the silylation agent through the polymer (Case II diffusion) and the chemical reaction with the OH-resin groups forming resin bonded silicon. Figure 6 shows the calculated silylation and swelling profiles in the resist after 60 sec of silylation using the extended DESIM model and a modified string algorithm [11] to simulate the time evolution of the silylation front. It is well known that the swelling is an effect due to the incorporation of larger silicon agent molecules into the resist surface areas and its depth can be set as a ratio of the silylation depth (in this simulation it is set to 30%).

The calculated silicon depth in the NUV exposed regions of the resist is approximately 70nm. This corresponds well with the experimental data previously obtained for silicon incorporation in Shipley SPR500-series resists using Secondary Ion Mass (SIM) spectrometry [12].

In the last PRIME step, a final O_2 -RIE dry development is used to develop structures by means of the oxidation of the resist and the incorporated silicon. The oxidation of the unsilylated areas in the former e-beam exposed region in the middle of the structure (Fig. 6) will result in reaction products like CO_2 and H_2O . However, oxidation of the silylated areas will build a stable SiO-SiO₂ mask. Since the silicon oxide has very low oxygen etch rate, it will act as a build-in mask for the underlying resist layer, while all other resist regions will be etched away.

The two step O_2 -RIE dry development process was modeled using string algorithm for topographic substrate and a factor of anisotropy [10]. In the first step, a thin surface layer is removed (resist stripping) to avoid any unwanted silicon incorporation in the crosslinked areas, while the second stage consists of anisotropic dry development. The factor of anisotropy can be varied between 0.5 and 1 to model all possible dry development profiles for various rf power and partial pressure during the process [10].

The obtained resist silylation profile shown in Fig 6 was taken as an input for the dry development

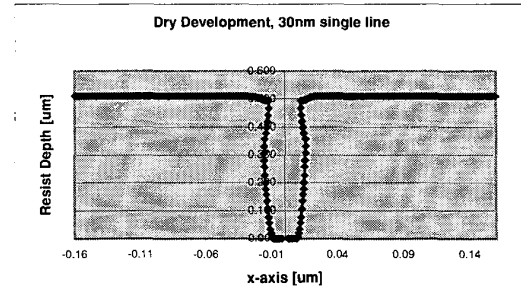
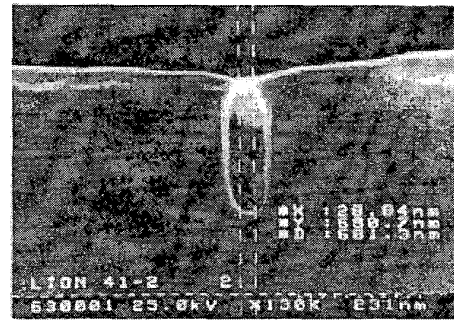
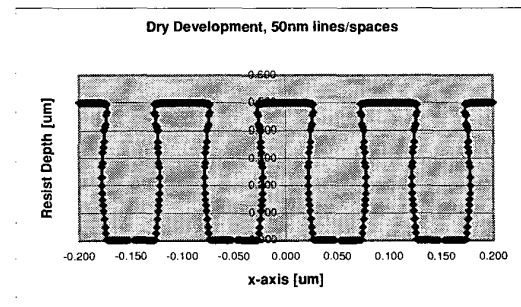


Fig.7: Dry development simulation, 30nm line.

Fig.8: 30nm line after PRIME, Bauch *et al.* [13].

modelling process. Figure 7 shows the simulated 30nm dry developed resist profile after 10 min etching time with a degree of anisotropy of 0.7 and 10 nm resist stripping. Figure 8 shows the experimentally obtained dry developed profile for 30 nm line reported by Bauch *et al.* [13], using the PRIME process in 0.5 μm thick DNQ/novolak based resist. Our simulated profile (Fig. 7) shows the same mushroom shape with slight blowing at the surface, which can be attributed to the low mean free path on the ions during the O_2 development.

Fig.9: 50nm lines/spaces in 0.5 μm Shipley SPR505A.

Simulations for 50nm lines/spaces in 0.5 μm Shipley SPR505A resist were performed using similar e-beam

& NUV exposures settings. The dry development process was modeled with the same value of anisotropy (0.7). However, this simulation setting agreed well with the experimental result shown above (Fig. 8). Figure 9 shows the modeled dry development profiles of 50nm lines/spaces after etching time of 11 min with 20nm resist stripping.

4. Silylation Characterization of SPR505A

The silylation step in PRIME process with Shipley SPR505A resist has been experimentally characterized using Fourier Transform – Infrared (FT-IR) spectroscopy to measure the silicon uptake in the resist. The silylation process was performed in liquid-phase, using HMCTSx (hexamethylcyclotrisiloxane) as a silylation agent.

Shipley SPR505A resist was spin coated at 4000rpm on Si-wafers and prebaked at 90°C for 60sec on hotplate, giving a nominal film thickness of 0.5µm. The electron-beam exposure of the samples was performed using a modified Jeol JSM-840 SEM at 30 KeV acceleration voltage and exposure doses between 25-100µC/cm². To optimize the silylation characterization of SPR505A resist, exposures were conducted on large areas in the (µm)² region. The subsequent near UV flood exposure was carried out on a broadband NUV Karl Suss MJB 21 mask aligner with dose of 250mJ/cm². The wafers were postexposure baked at 105°C for 60sec on hotplate.

The liquid-phase silylation was performed at room temperature by immersing the resist-coated wafers in solution containing HMCTSx, a bi-functional silylation agent, PGMEA (propylene-glycol-methyl-ether-acetate), a resist solvent and diffusion promoter, and xylene (HMCTSx solvent). At the end, the samples were submerged in xylene for 15 sec to stop the silylation reaction, rinsed with DI-water and dried with O₂.

The expected silylation reaction between HMCTSx and the phenolic-OH groups of the novolak resin is shown in Figure 10. The Si(CH₃)₂ group of the silylation agent replaces the hydrogen atom in the OH-group to form a resin-bonded silicon.

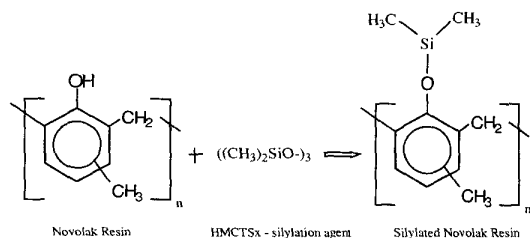


Fig.10: HMCTSx-phenol silylation reaction.

The silicon uptake in SPR505A resist was quantified by measuring the integrated IR absorbance of Si-C bond deformation peak (1280cm⁻¹-1240cm⁻¹). A new method has been developed for those measurements as we first apply baseline corrections and normalization of the collected IR spectra to avoid any fluctuations in resist thickness.

Figure 11 shows the FT-IR difference spectrum, which is before and after 60sec silylation for the NUV exposed resist regions. The spectrum clearly shows the presence of the Si-C bond stretching vibration at 1264cm⁻¹. The silylation mixture composition was optimised to 20%-5%-75% (HMCTSx-PGMEA-Xylene), showing the highest silicon uptake with changing the concentration of the diffusion promoter from 0% to 20% (Fig.12). It is noticeable that small amount of PGMEA greatly enhances the silylation, while concentration higher than 15% will lead the resist to be dissolved.

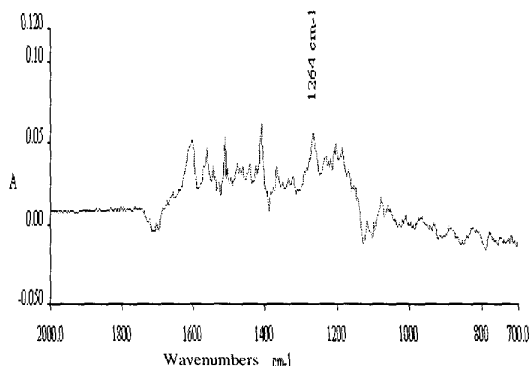


Fig.11: FT-IR difference spectrum for the 60sec silylated resist (after silylation-before silylation).

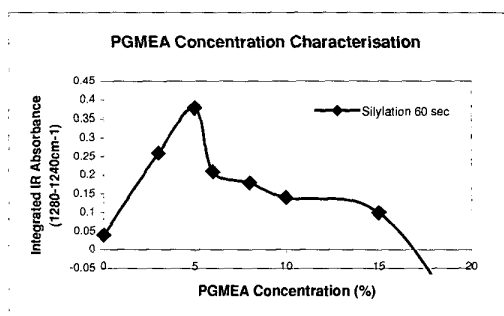


Fig.12: Incorporated silicon content as a function for various PGMEA concentrations.

The effect of crosslinking the SPR505A resist under electron beam exposure was investigated to estimate the required dose so that to prevent silylation in the e-beam exposed areas. The relationship between electron

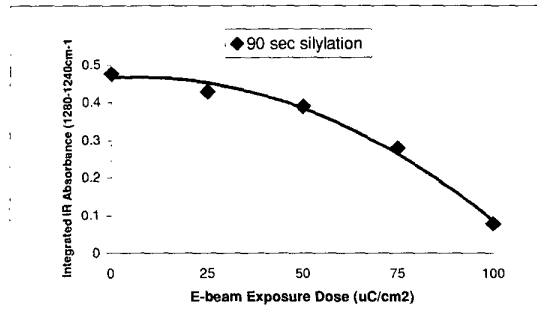


Fig.13: The relation between e-beam exposure dose and silylation quantity.

beam exposure dose and the silicon uptake in the irradiated resist areas is shown in Figure 13. The resist samples were irradiated with different e-beam doses (25-100 $\mu\text{C}/\text{cm}^2$) and silylated for 90sec, as the integrated IR absorbance peak (1280 cm^{-1} -1240 cm^{-1}) was monitored. Experiments show that an e-beam dose larger than 50 $\mu\text{C}/\text{cm}^2$ effectively cross-links the resist, thus decreasing significantly the silicon uptake during silylation. To minimise the silicon incorporation in the e-beam irradiated areas, an exposure dose of 100 $\mu\text{C}/\text{cm}^2$ was chosen for the following experiments.

Finally, the silicon uptake for both the crosslinked and NUV exposed resist areas has been investigated as a function of the silylation time (Figure14). The integrated IR peak (1280 cm^{-1} -1240 cm^{-1}) increases at much faster rate in the NUV exposed regions than in the e-beam crosslinked regions, indicating a similar behaviour to that observed by Hutchinson *et al.* [14]. Hutchinson *et al.* used an eximer laser instead of electron beams to cross-links the resist. The contrast of the process as determined by the ratio of integrated IR absorbance of NUV exposed over crosslinked regions (Fig. 14), was found to be approximately 4.5:1, which is compared well with Hutchinson *et al.* [14].

Also the silicon incorporation over silylation time for the NUV exposed regions was found to be linear, indicating a Case II diffusion process. The same behaviour of the liquid-phase silylation process was also observed by Hartney *et al.* [15], using a similar silylation agent and Rutherford backscattering (RBS) analysis.

5. Summary

PRIME process with Shipley SPR505A resist has been investigated with both simulations and experiments. Modelling of the incorporated electron beam exposure, NUV flood exposure, silylation and O_2 -RIE dry

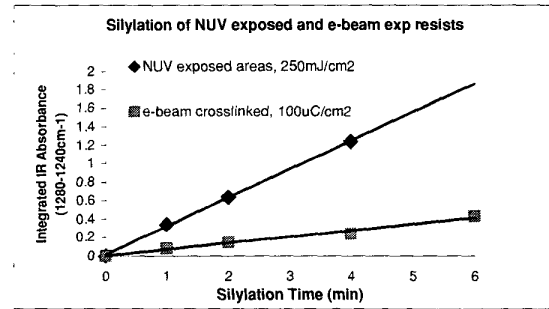


Fig.14: Silicon uptake versus time for the NUV exposed regions and e-beam crosslinked areas. Solid line is a linear fit to the experimental data.

development process has been presented. The experimental production of 50nm lines/spaces nanostructures had been validated by simulations. The simulated 30nm single line had been compared with the published experimental data, showing a good shape matching with the same degree of anisotropy. The simulations were performed using 0.02 μm Gaussian shaped electron beam with dose of 250 $\mu\text{C}/\text{cm}^2$, NUV exposure with dose of 50mJ/cm², 50sec silylation and 10min dry development. Moreover, the liquid-phase silylation process in PRIME with SPR505A was experimentally characterised using FT-IR. The silylation mixture composition was optimised to 20% HMCTS_x - 5% PGMEA -75% Xylene. The required e-beam dose was found to be greater than 50 $\mu\text{C}/\text{cm}^2$ so that to prevent silylation in the e-beam exposed areas. It was observed that the silicon uptake in the NUV exposed regions over time had a linear behaviour, indicating Case II diffusion process.

6. References

- [1] J. H. Levinson, Lithography: a look at what is ahead, in *Proc. SPIE Vol.4099*, pp.1-15, Nov 2000.
- [2] S. V. Postnikov, M. H. Somervell, C. L. Henderson, S. Katz, Top Surface Imaging through Silylation, in *Proc. SPIE Vol.3333*, pp.997-1008, June 2000.
- [3] C. Pierrat, S. Tedesco, F. Vinet, M. Lerme, B. Dal'Zotto, Positive Resist Image by Dry Etching: New Dry Developed Positive Working System for Electron Beam and Deep Ultraviolet Lithography, *J. Vac. Sci. Technol. B7(6)*: 1782-1786, Dec 1989.
- [4] SAMPLE 1.7a, University of California, Berkeley, March, 1989.
- [5] D. McDonagh, K.I. Arshak, A. Arshak, J. Braddell, SLITS simulator: modelling and simulation of ebeam/deep-ultraviolet exposure and

- silylation, *Optical Engineering*, 35(1): 277-283, 1996.
- [6] F. H. Dill, A. R. Neureuther, Modeling projection printing of positive photoresists, in *IEEE Trans. Electron Devices* ED-22(7): 456-464, 1975.
 - [7] C. Mack, Analytical expression for the standing wave intensity in photoresist, *Appl. Opt.* Vol.25: 1958-11961, 1986.
 - [8] C. Mack, A diffusion model for post exposure bake, *PROLITH User's Guide*, 1988.
 - [9] Data sheet Shipley SPR505A photoresist.
 - [10] B. Mathur, K. Arshak, D. McDonagh, DESIM: a simulator for the DESIRE process, in *Proc. SPIE Vol.2195*, pp 497-505, 1994.
 - [11] K. Arshak, D. McDonagh B. Mathur, A. Arshak, Topography simulation in photolithography using finite element analysis and a modified string algorithm, in *NASCODE X Trans, COMPEL* 13(4), pp 871-878, 1994.
 - [12] J. R. Schinagl, Development of a Design Process for Phase Shift Mask Manufacture, M.Eng. Thesis, University of Limerick, 1998.
 - [13] L. Bauch, M. Bottcher, U. Jagdhold, in *Proc. 10th Int. Conf. Photopolymers*, pp. 343-347, 1994.
 - [14] J. Hutchinson, K. Kalpakjian, R. Schenker, W. Oldham, Evaluation of Liquid Silylated Resists for 213nm Exposure, in *Proc. SPIE Vol.1925*, pp 414-425, 1993.
 - [15] M. Hartney, R. Kunz, L. Eriksen, D. C. La Tulipe, *Optical Engineering*, 32(10): 2382-2387, 1993.